A photonic ultra-wideband pulse generator based on relaxation oscillations of a semiconductor laser

Yu, Xianbin; Gibbon, Timothy Braidwood; Pawlik, Michal; Blaaberg, Søren ; Tafur Monroy, Idelfonso

Published in:
Optics Express

Link to article, DOI:
10.1364/OE.17.009680

Publication date:
2009

Document Version
Publisher's PDF, also known as Version of record

A photonic ultra-wideband pulse generator based on relaxation oscillations of a semiconductor laser

Xianbin Yu*, Timothy Braidwood Gibbon, Michal Pawlik, Søren Blaaberg, and Idelfonso Tafur Monroy

DTU Fotonik, Department of Photonics Engineering, Technical University of Denmark, Ørsteds Plads, DK-2800 Kgs. Lygnby, Denmark.
**Corresponding author: xiyu@fotonik.dtu.dk*

Abstract: A photonic ultra-wideband (UWB) pulse generator based on relaxation oscillations of a semiconductor laser is proposed and experimentally demonstrated. We numerically simulate the modulation response of a direct modulation laser (DML) and show that due to the relaxation oscillations of the laser, the generated signals with complex shape in time domain match the Federal Communications Commission (FCC) mask in the frequency domain. Experimental results using a DML agree well with simulation predictions. Furthermore, we also experimentally demonstrate the generation of FCC compliant UWB signals by externally injecting a distributed feedback (DFB) laser.

OCIS codes: (060.4510) Optical communications; (060.5625) Radio frequency photonics; (320.5550) Pulses; (250.4745) Optical processing devices; (250.5960) Semiconductor lasers.

References and links

1. D. Porcine, P. Research and W. Hirt, "Ultra-wideband radio technology: potential and challenges ahead," IEEE Commun. Mag. **41**, 66-74 (2003).
2. R. Llorente, T. Alves, M. Morant, M. Beltran, J. Perez, A. Cartaxo and J. Marti, "Ultra-wideband radio signals distribution in FTTH networks," IEEE Photon. Technol. Lett. **20**, 945-947 (2008).
3. W. P. Lin and Y. C. Chen, "Design of a new optical impulse radio system for ultra-wideband wireless communications," IEEE J. Sel. Top. Quantum Electron. **12**, 882–887 (2006).
4. J. Yao, F. Zeng and Q. Wang, "Photonic Generation of Ultrawideband Signals," J. Lightwave Technol. **25**, 3219-3235 (2007).
5. C. Wang, F. Zeng and J. P. Yao, "All-fiber ultra wideband pulse generation based on spectral shaping and dispersion-induced frequency-to-time conversion," IEEE Photon. Technol. Lett. **19**, 137–139 (2007).
6. Q. Wang and J. Yao, "An electrically switchable optical ultrawideband pulse generator," J. Lightwave Technol. **25**, 3626-3633 (2007).
7. Q. Wang, F. Zeng, S. Blais and J. Yao, "Optical ultrawideband monocycle pulse generation based on cross-gain modulation in a semiconductor optical amplifier," Opt. Lett. **31**, 3083-3085 (2006).
8. H. Chen, M. Chen, C. Qiu, S. Xie, "A novel composite method for ultra-wideband doublet pulses generation," IEEE Photon. Technol. Lett. **19**, 2021-2023 (2007).
9. J. Li, S. Fu, K. Xu, J. Wu, J. Lin, M. Tang and P. Shum, "Photonic ultrawideband monocycle pulse generation using a single electro-optic modulator," Opt. Lett. **33**, 288-290 (2008).
10. J. Dong, X. Zhang, J. Xu, D. Huang, S. Fu and P. Shum, "Ultrawideband monocycle generation using cross-phase modulation in a semiconductor optical amplifier," Opt. Lett. **32**, 1223-1225 (2007).
11. W. P. Lin and J. Y. Chen, "Implementation of a new ultrawide-band impulse system," IEEE Photon. Technol. Lett. **17**, 2418-2420 (2005).
12. M. Abtahi, J. Magné, M. Mirshafiei, L. A Rusch and S. LaRochelle, "Generation of power-efficient FCC-compliant UWB waveforms using FBGs: analysis and experiment," J. Lightwave Technol. **26**, 628-635 (2008).
13. Q. Wang, J. Yao, "UWB doublet generation using nonlinearly biased electro-optic intensity modulator," Electron. Lett. **42**, 1304-1305 (2006).
14. T. Kawanishi, T. Sakamoto and M. Izutsu, "Ultra-wide-band radio signal generation using optical frequency-shift-keying technique," IEEE Microwave Wirel. Compon. Lett. **15**, 153–155 (2005).
15. V. Torres-Company, K. Prince and I. T. Monroy, "Fiber transmission and generation of ultrawideband pulses by direct current modulation of semiconductor lasers and chirp-to-intensity conversion," Opt. Lett. **33**, 222-224 (2008).

#107937 - $15.00 USD Received 25 Feb 2009; revised 13 May 2009; accepted 17 May 2009; published 26 May 2009

16. H. Sheng; P. Orlik,; A. M. Haimovich, L. J. Cimini Jr., J. Zhang, "On the Spectral and Power Requirements for Ultra-Wideband Transmission," IEEE International Conference on Communications (ICC2003) **1**, 738 – 742 (2003).
17. G. P. Agrawal, *Fiber optic communication systems (second edition)* (John Wiley & Sons, Inc. 1997), pp. 110-122.

1. Introduction

Ultra-wideband (UWB) is a promising short range wireless communication technology due to its very low required signal-to-noise ratio (SNR) operation and wide bandwidth within unlicensed spectrum (3.1-10.6 GHz) specified by the Federal Communications Commission (FCC) [1]. However, this technique is limited in coverage to its immediate surrounding area (up to 10 m or 30 feet) because of its low radiation power. On the other hand, optical fiber based access technology such as fiber-to-the-customer-premises (FTTCP) has the well-known advantages of low loss, large bandwidth, long reach and is currently being deploying worldwide. Thus UWB-over-fiber is attractive as a promising approach to extend the reach of UWB systems and to consolidate wireless personal access networks with FTTCP [2, 3]. In this scenario, simple ways to generate UWB signals by photonic means are highly desired.

A number of different pulse shapes have been designed to meet the FCC requirements, and most of them are based on derivatives of a Gaussian pulse shape. The first derivative of a Gaussian pulse is referred to as a monocycle, and the second derivative is known as a doublet. Recently, many methods have been proposed to generate UWB signals in the optical domain [4-15]. Typically, these methods can be divided into two broad classes: time delay and nonlinear signal processing. In the first method, two Gaussian pulses with π phase difference are combined at the receiver side by controlling the delay time between the pulses [4]. Thus far, numerous implementations for optical delay lines have been exploited and applied for the generation of UWB signals, such as fiber Bragg grating (FBG) [5, 6, 7], differential group delay (DGD) module [8], dispersion medium [9], semiconductor optical amplifier [10], amongst others. The second method is based on the nonlinear processing capability of some electrical or photonic components, after which the derivative of the Gaussian pulse is achieved. For example, a microwave differentiator [11], nonlinear pulse shaping of FBG [12] and nonlinear modulation of electro-optical modulators [13, 14] have been proposed. Meanwhile, a photonic UWB generator based on direct current modulation of a laser and chirp-to-intensity conversion has also been experimentally demonstrated [15]. Most of these efforts focus on the generation of monocycle or doublet pulses. Moreover, the studies in [12, 16] show the monocycle and monocycle based Gaussian pulses hardly follow the FCC requirements, and that one way to overcome this limitation is to generate higher-order (up to fifth-order) derivatives of the Gaussian pulse with complex shape.

In this paper, we propose a photonic method to generate high-order Gaussian derivative UWB pulses with complex shape by utilizing the relaxation oscillations of a semiconductor laser. We numerically simulate the modulation response of a directly current modulated laser (DML) and experimentally validate the simulation results. Similarly, a photonic UWB generator by optical external injecting of a distributed feedback laser (DFB) is also proposed and experimentally demonstrated.

2. Modulation response of semiconductor laser

The block diagram for generation of UWB pulses by using a DML is shown in Fig. 1. A 12.5 Gbit/s pulse pattern from a pattern generator is used to directly modulate a DML, whose operation point is set by using a direct current (DC) bias.

When a semiconductor laser is directly modulated by a current *I(t),* its modulation response can be described by the following set of rate equations, which show the interaction of photons and electrons within the active region [17].

#107937 - $15.00 USD Received 25 Feb 2009; revised 13 May 2009; accepted 17 May 2009; published 26 May 2009

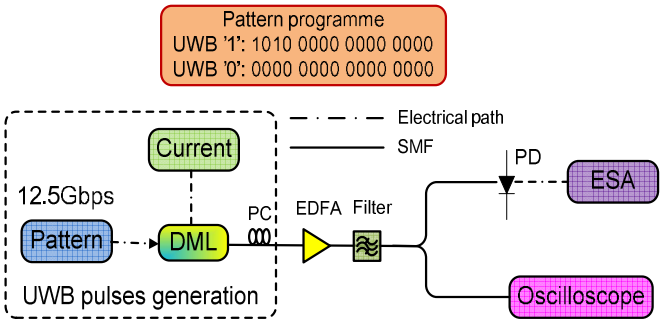

Fig. 1. Photonic UWB generator based on a DML. DML: direct modulation laser, PC: polarization controller, EDFA: Erbium-doped fiber amplifier, SMF: single mode fiber, PD: photodiode, ESA: electrical spectrum analyzer.

$$\frac{dP}{dt} = GP + R_{sp} - \frac{P}{\tau_p} \tag{1}$$

$$\frac{d\varphi}{dt} = \frac{1}{2}\alpha[G - \frac{P}{\tau_p}] \tag{2}$$

$$\frac{dN}{dt} = \frac{I}{qV} - \frac{N}{\tau_c} - GP \tag{3}$$

where P is the photons density, N is the carrier density, G is the net rate of stimulated emission, R_{sp} is the rate of spontaneous emission into the lasing mode, τ_p is the photon lifetime, φ is the phase, α is the linewidth enhancement factor, τ_c is the carrier lifetime, q is the charge of an electron, and V is the volume of active region. Eqs. (1) and (2) represent the light emitting characteristics of the semiconductor laser taking into account the loss of photons inside the laser cavity, and Eq. (3) indicates the rates at which carriers are created or destroyed inside the active region.

The input time-dependent current can be expressed as

$$I(t) = I_{bias} + I_{\mathrm{mod}} f_{\mathrm{mod}}(t) \tag{4}$$

where I_{bias} is DC bias current, $f_{mod}(t)$ represents the shape of modulation pulse and I_{mod} is the modulation current.

Generally, in the case of large signal modulation, in which the laser is biased above threshold (I_{bias}>I_{th}), and the amplitude of modulation current I_{mod} is close to I_{bias}-I_{th}, the laser output light is also modulated. Meanwhile, the carrier and photon density inside the laser active region change with time as well. In particular, relaxation oscillations play an important role in governing the dynamic response of the semiconductor laser. Due to the relaxation oscillations, the output optical pulse after modulation does not exhibit the same shape as the driving electrical pulse. Simulation and experimental results of laser modulation response and generation of UWB pulse are presented in the following sections.

3. Simulation results

By defining the input current and computing the rate Eqs. (1)-(3), the modulation response of the semiconductor laser can be studied by calculating the rate equations numerically.

In our case, the UWB generator display in the dashed frame in Fig. 1 is simulated. The parameters used in the simulation are listed in Table 1. To make the simulation as accurate as possible, some parameters used in the simulation are extracted from measurements. These

#107937 - $15.00 USD Received 25 Feb 2009; revised 13 May 2009; accepted 17 May 2009; published 26 May 2009

include the laser threshold, bit rate and laser DC bias current. Furthermore, the input electrical modulating 16-bit pattern sequence '0101 1111 1111 1111' is chosen. In our model, the laser DC bias current is a positive value, but a negative current is used in the experiment. Therefore, the 16-bit 12.5 Gbit/s pattern sequence has to be '0101 1111 1111 1111' in the simulation, which is the logical equivalent pattern of '1010 0000 0000 0000' used in the experiment. It is noted that double ones in the logical pattern are set to obtain higher-order UWB pulses than those reported in [15]. As seen in Fig. 2(a), the amplitude of modulation current is 10mA and the duration of one electrical bit is 80 ps.

Table 1. The Parameters used in the simulation

Parameters	Values[unit]
I_{bias} (laser DC bias current)	-34.85 [mA]
I_{th} (laser threshold)	-21 [mA]
α (linewidth enhancement factor)	3
τ_p (photon lifetime)	4.34e-12 [s]
τ_c (carrier lifetime)	4e-10 [s]
q (electron charge)	1.6e-19 [C]
bit rate	12.5 [Gbit/s]

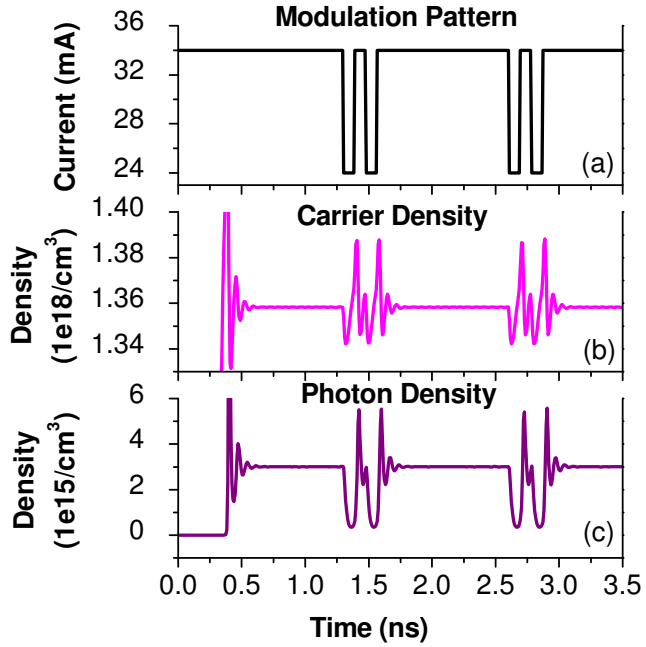

Fig. 2. Simulation results in the case of using a modulation pattern sequence '0101 1111 1111 1111'. (a) the input modulation pattern with 10 mA current, (b) the change of carrier density with time, (c) the change of photon density with time.

The variation of input current with time causes the change in the carrier concentration in the semiconductor, as shown in Fig. 2(b). This implies a change in the photon density inside the cavity, as shown in Fig. 2(c). Due to the turn-on delay, stimulated emission does not appear until carrier concentration has reached the threshold emission value. In particular, it is noticed that the total chirp of the signal is composed of two parts: transient chirp and adiabatic chirp. The transient chirp expresses the frequency variation due to time power variation of the signal and the adiabatic chirp expresses the frequency change of the emitted signal due to

#107937 - $15.00 USD Received 25 Feb 2009; revised 13 May 2009; accepted 17 May 2009; published 26 May 2009

changes of the semiconductor refractive index and carrier density. As the DFB laser is biased close to the laser threshold, the total resultant frequency chirp is composed mostly of the transient chirp. The output pulses are proportional to the photon density, and hence the output pulses have same shapes as shown in Fig. 2(c) in the time domain, which represents most of the chirp in the system due to the relaxation oscillations. The output pulses have double-valley shapes due to two zeros in the original electrical driving pattern. Meanwhile, two intensive overshooting peaks and some subsequent weak vibrations caused by the relaxation oscillations can be observed. The small distortion on the second valley is because the laser attempts to relax before the arrival of the second '0', which prevents the relaxation oscillations. Due to the presence of the relaxation oscillations, pulses with complex shapes (close to the shapes of high-order Gaussian pulses) are generated. The frequency spectra of the generated signal as shown in Fig. 3 are obtained by applying a Fourier transform to the signals in time domain. We can notice that this spectrum has a repetition rate of 781 MHz, and a peak value at 5.7 GHz is obtained in the frequency band 3-9 GHz.

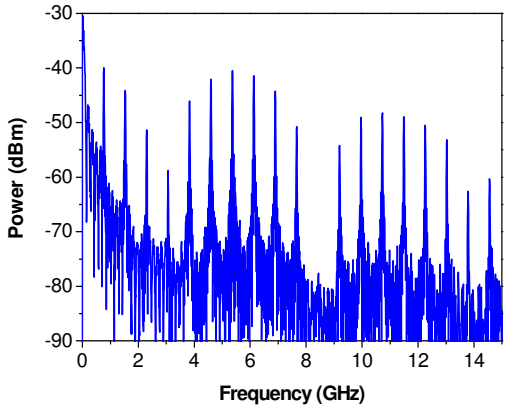

Fig. 3. The simulated output frequency spectra corresponding to the pulses in Fig. 2(d).

4. Experimental validations and discussions

4.1 Direct modulation laser

Firstly, an experimental system based on a DML is built to validate the simulation results, as shown in Fig. 1. The UWB generation devices in the dashed frame have been previously described in section 2. After UWB signal generation an Erbium-doped fiber amplifier (EDFA) is employed to amplify the modulated optical pulses, followed by an optical filter to reject amplified spontaneous emission (ASE) noise. At the receiver side an optical oscilloscope is used to display the generated pulses in time domain, and the signals in frequency domain are also observed on an electrical spectrum analyzer (ESA) after a photodiode (PD) with 12 GHz 3 dB bandwidth.

The operation characteristic of the DML is plotted in Fig. 4. It indicates that the threshold current value is around -21 mA. Above this threshold, the laser has a linear response. In the experiment, the laser is based at -34.85 mA and the average output power is measured to be 0.54 mW. The output signals in time domain and frequency domain are shown in Fig. 5. We can notice that the generated signals with complex shapes agree well with the simulated results. Assuming that a "1" UWB bit consists of the 12.5 Gb/s 16-bit sequence "1010 0000 0000 0000" and a "0" UWB bit consists of a sequence of 16 consecutive "0" 12.5 Gbit/s bits, on-off keying UWB signals will be obtained. Limited by the length of the UWB bit pattern, the spectra in frequency domain shown in Fig. 5(b) show some discrete frequency

#107937 - $15.00 USD Received 25 Feb 2009; revised 13 May 2009; accepted 17 May 2009; published 26 May 2009

components with a repetition rate of 781 MHz. The spectral envelope has a central frequency of 5.7 GHz with a 10 dB bandwidth of 4.5 GHz, from 3.5 to 8 GHz. Therefore, the fractional bandwidth is approximately 78%, which meets the FCC minimum requirement of 20%.

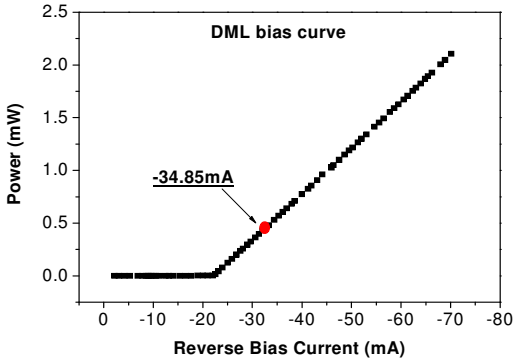

Fig. 4. Bias characteristics of DML used in the experiment.

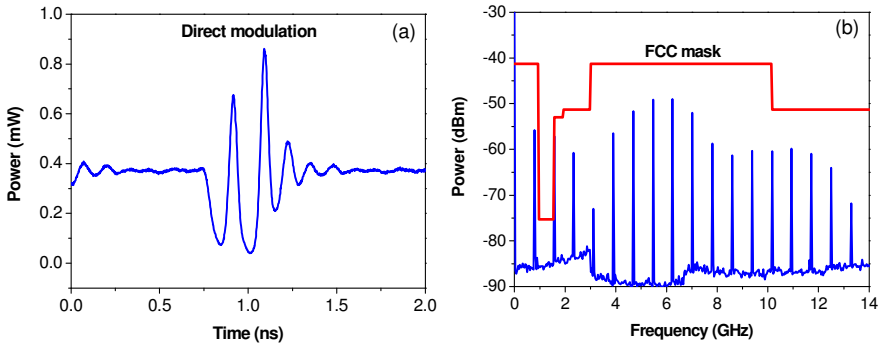

Fig. 5. The measured output UWB signals in time domain and frequency domain as obtained by directly modulating the DML. (a) pulses in time domain, (b) frequency spectra of the signals in Fig. 5(a), as well as the FCC requirements mask.

4.2 External injection of a laser

An alternative approach to UWB generation is to optically inject a data signal into a DFB laser instead of using direct current modulation. The experimental setup is shown in Fig. 6. In this case, the 12.5 Gbit/s 16-bit pattern sequence '1010 0000 0000 0000' is used to drive a Mach-Zehdner modulator (MZM), whose input optical signal is derived from a continuous-wave laser (CW). An optical circulator (OC) is employed to separate the lightwave launched into the DFB from the DFB output signal. An EDFA is used to amplify the signals prior to photodetection. An optical spectrum analyzer is used to observe the signals in optical domain. An ESA and an oscilloscope are employed to analyze the electrical signals in frequency domain and in time domain, respectively.

Due to the cross gain modulation (XGM) inside the DFB laser, the emitting wavelength of the DFB is modulated by the original pattern. In order to improve the XGM modulation efficiency, the CW wavelength is chosen to correspond to one of the DFB side grating resonance wavelengths. The optical spectra are shown in the right of Fig. 6, as well as the transfer function of the used optical filter. In this experiment, the CW wavelength is at 1553.6 nm, and the DFB wavelength is at 1551.4 nm. We can notice that the UWB pulses comprise only of the DFB wavelength after the filter. The optical pulses modulated on the

#107937 - $15.00 USD Received 25 Feb 2009; revised 13 May 2009; accepted 17 May 2009; published 26 May 2009

CW lightwave are measured at the output of the MZM biased at quadrature point, as displayed in Fig. 7. The original pattern '1010 0000 0000 0000' can clearly be observed.

In the experiment, the optical filter performs two functions: rejecting the CW wavelength and shaping the output pulse. The generated UWB signals are shown in Fig. 8. The time trace in Fig. 8(a) is very similar to the case in Fig. 5(a). The spectra in frequency domain meet the FCC requirement as well, and have a central frequency of 6.3 GHz with a 10 dB bandwidth of 3.8 GHz, from 4.3 to 8.1 GHz. The fractional bandwidth is approximately 61%.

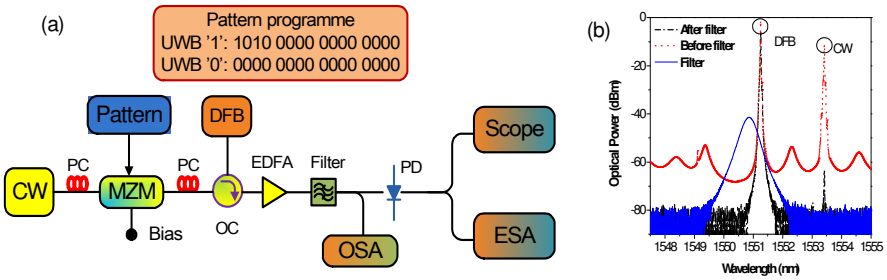

Fig. 6. (a). the photonic UWB generator by externally injecting a DFB laser. CW: continuous wave laser, MZM: Mach-Zehdner modulator, DFB: distributed feedback laser, OC: optical circulator, OSA: optical spectrum analyzer. (b) the measured optical spectra before and after the optical filter, as well as the transfer function of optical filter used in the experiment.

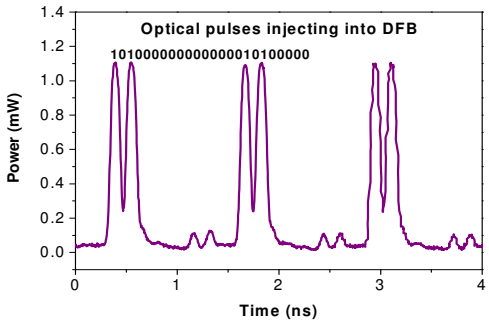

Fig. 7. the measured pulses after the MZM when a 16-bit 12.5 Gbit/s sequence '1010 0000 0000 0000' is applied.

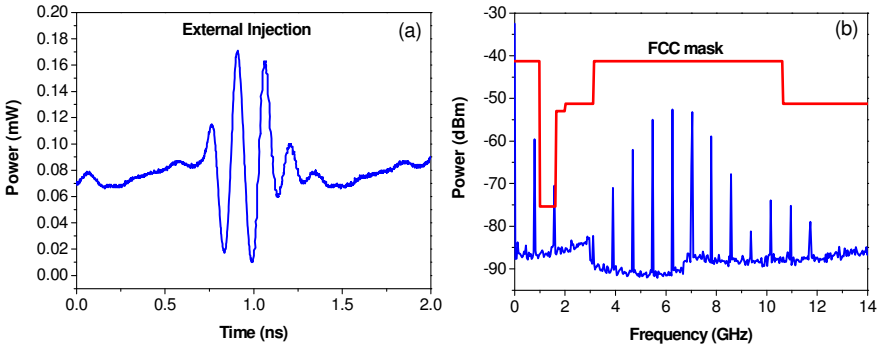

Fig. 8. The measured output UWB signals in time domain and frequency domain by externally injecting the DFB laser. (a) pulses in time domain, (b) frequency spectra of signals in Fig. 8(a), as well as the FCC requirements.

#107937 - $15.00 USD Received 25 Feb 2009; revised 13 May 2009; accepted 17 May 2009; published 26 May 2009

5. Conclusions

Generation of UWB signals by utilizing the relaxation oscillations of an uncooled semiconductor laser is theoretically and experimentally demonstrated. We numerically simulate the modulation response of the DML by applying a 12.5 Gbit/s 16-bit sequence '1010 0000 0000 0000'. The generated signal has a complex shape in time domain. Furthermore, an experiment based on a direct current modulation of a DFB laser validates the simulation predictions. The generated pulse in the experiment agrees with the simulated and its frequency spectrum is compliant with the FCC mask. Another approach is to use optical external injection of a DFB laser. In this case we also experimentally demonstrate that the generated UWB signals have high-order shapes in time domain and meet the requirements of the FCC mask in frequency domain. Our proposed scheme for generation of UWB signals is very simple and cost effective, and has potential application in high-speed UWB FTTCP transmission systems.

#107937 - $15.00 USD Received 25 Feb 2009; revised 13 May 2009; accepted 17 May 2009; published 26 May 2009